New molecular and therapeutic insights into canine diffuse large B-cell lymphoma elucidates the role of the dog as a model for human disease

Luca Aresu,[1] Serena Ferraresso,[2] Laura Marconato,[3] Luciano Cascione,[4,5] Sara Napoli,[4] Eugenio Gaudio,[4] Ivo Kwee,[4,5,6] Chiara Tarantelli,[4] Andrea Testa,[7] Chiara Maniaci,[7,8] Alessio Ciulli,[7] Petra Hillmann,[9] Thomas Bohnacker,[10] Matthias P. Wymann,[10] Stefano Comazzi,[11] Massimo Milan,[2] Fulvio Riondato,[1] Giulia Dalla Rovere,[2] Mery Giantin,[2] Diana Giannuzzi,[2] and Francesco Bertoni[4*]*

[1]Dipartimento di Scienze Veterinarie, Università degli Studi di Torino, Italy; [2]Dipartimento di Biomedicina Comparata e Alimentazione, Università degli Studi di Padova, Italy; [3]Centro Oncologico Veterinario, Sasso Marconi, Italy; [4]Università della Svizzera Italiana, Institute of Oncology Research, Bellinzona, Switzerland; [5]Swiss Institute of Bioinformatics, Lausanne, Switzerland; [6]Dalle Molle Institute for Artificial Intelligence, Manno, Switzerland; [7]Division of Biological Chemistry and Drug Discovery, School of Life Sciences, University of Dundee, Scotland, United Kingdom; [8]Department of Chemistry, Chemistry Research Laboratory, University of Oxford, England, United Kingdom; [9]PIQUR Therapeutics AG, Basel, Switzerland; [10]Department of Biomedicine, University of Basel, Switzerland and [11]Dipartimento di Medicina Veterinaria, Università degli Studi di Milano, Italy

Correspondence: LUCA ARESU. FRANCESCO BERTONI.
luca.aresu@unito.it/frbertoni@mac.com
doi:10.3324/haematol.2018.207027

New molecular and therapeutic insights into canine diffuse large B cell lymphoma elucidates the role of the dog as a model for human disease

Luca Aresu [1*], Serena Ferraresso [2], Laura Marconato [3], Luciano Cascione [4,5], Sara Napoli [4], Eugenio Gaudio [4], Ivo Kwee [4,5,6], Chiara Tarantelli [4], Andrea Testa [7], Chiara Maniaci [7,8], Alessio Ciulli [7], Petra Hillmann [9], Thomas Bohnacker [10], Matthias P. Wymann [10], Stefano Comazzi [11], Massimo Milan [2], Fulvio Riondato [1], Giulia Dalla Rovere [2], Mery Giantin [2], Diana Giannuzzi [2], Francesco Bertoni [4*]

[1] Dipartimento di Scienze Veterinarie, Università degli Studi di Torino, Torino, Italy;
[2] Dipartimento di Biomedicina Comparata e Alimentazione, Università degli Studi di Padova, Padova, Italy;
[3] Centro Oncologico Veterinario, Sasso Marconi, Italy;
[4] Università della Svizzera italiana (USI), Institute of Oncology Research (IOR), Bellinzona, Switzerland;
[5] Swiss Institute of Bioinformatics (SIB), Lausanne, Switzerland;
[6] Dalle Molle Institute for Artificial Intelligence (IDSIA), Manno, Switzerland;
[7] Division of Biological Chemistry and Drug Discovery, School of Life Sciences, University of Dundee, Dundee, Scotland, United Kingdom;
[8] Department of Chemistry, Chemistry Research Laboratory, University of Oxford, Oxford, England, United Kingdom;
[9] PIQUR Therapeutics AG, Basel, Switzerland;
[10] Department of Biomedicine, University of Basel, Basel, Switzerland;
[11] Dipartimento di Medicina Veterinaria, Università degli Studi di Milano, Milano, Italy.

Online Supplementary Methods

DLBCL cohort of primary samples

Dogs with newly diagnosed, previously untreated, multi-centric DLBCL of any World Health Organization (WHO) clinical stage admitted to the Centro Oncologico Veterinario (Sasso Marconi, Italy) were included in the study. To be eligible for enrollment, dogs were required to undergo a complete staging work-up, consisting of history and physical examination, complete blood cell count with differential, serum biochemistry profile, thoracic radiographs and abdominal ultrasound, cytological evaluation of liver and spleen regardless of the ultrasonographic appearance, and immunophenotype determined by flow cytometry on a lymph node aspirate, peripheral blood and bone marrow aspirate. Before the initiation of therapy, all dogs underwent lymphadenectomy to confirm DLBCL histotype by routine histology and immunohistochemistry (CD3, CD20, CD79 and PAX5) and to provide material for the vaccine generation [1]. A portion of the neoplastic lymph node was always RNA-later preserved and stored at -80°C. In addition to tumor samples, skin punch biopsies were obtained from all the dogs included in the study to provide matched paired normal tissue. Dogs' owners were required to give written informed consent. Approval for this study was granted by the Ministero dell'Istruzione, dell'Universita' e della Ricerca Ethical Board (Number RBSI14EDX9).

Dogs comprised 39 (78%) purebred and 11 (22%) crossbred dogs; among the 39 purebred dogs, the three more frequent were German shepherds (*N* 7), Golden retrievers (*N* 4) and Rottweiler (*N* 3). There were 26 (52%) males (of which four were castrated), and 24 (48%) females (of which 15 were spayed). The median age was 7.5 years (range 3-15 years) and the median weight was 28.9 kg (range 4.5-81.3 kg). Based on the WHO staging system, two (4%) dogs had stage III disease, 15 (30%) had stage IV disease, and 32 (64%) had stage V disease. Among dogs with stage V disease, 25 (78.1%) dogs had PB and BM involvement, eight (41.2%) dogs had BM involvement, and one dog had PB involvement. Forty-three (86%) dogs had no symptoms at presentation (substage a), whereas 17 (14%) did (substage b). Twenty-six (52%) dogs had an increased LDH activity. Overall, 14 (28%) dogs received prednisone at a dose of 0.5-1.0 mg/kg before being referred. Thirty (60%) dogs were treated by means of a CHOP-based protocol with the incorporation of APAVAC

immunotherapy, as previously described. Briefly, chemotherapy consisted of L-Asparaginase (week 1), Vincristine (week 2, 3, 4, 13), Cyclophosphamide (week 2, 13), Doxorubicin (week 7, 16), Lomustine (week 10, 19), and prednisone (week 1 through 20). Dogs also received an intradermal injection of an autologous vaccine on weeks 4, 5, 6, 7, 12, 16, 20, and 24. Twenty (40%) dogs were treated with CHOP-based chemotherapy only.

Control samples were derived from lymph nodes of 11 dogs that were clinically normal both at physical examination and blood profile. A portion of lymph nodes was snap frozen in O.C.T immediately after sampling. Five-micrometer thick frozen sections were obtained, stained with hematoxylin and eosin, and immunostained for CD20 and CD3 to guide the dissection. The follicular B-cell compartment was isolated by laser capture microdissection using the Arcturus PixCell II system. Both DNA and RNA were extracted as follow.

The second independent series of 44 cDLBCLs comprised 30 (68%) purebred and 14 (32%) crossbred dogs; among the 30 purebred dogs, the three more frequent were Labrador retrievers (*N* 8), Golden retrievers (*N* 5) and Dogo Argentino (*N* 4). There were 22 (50%) males (of which six were castrated), and 22 (50%) females (of which 20 were spayed). The median age was 9 years (range 4-14 years) and the median weight was 26-7 kg (range 6.5-70.5 kg). Based on the WHO staging system, one (2%) dog had stage III disease, 20 (45%) had stage IV disease, and 23 (52%) had stage V disease. All the dogs were treated by means of a CHOP-based protocol with the incorporation of APAVAC immunotherapy,

RNA/DNA isolation and sequencing

Total RNA and DNA were extracted from all the samples, using the AllPrep DNA/RNA Mini Kit (Qiagen, Hilden, Germany) according to the manufacturer's instructions. DNA concentration and quality were measured by Qubit fluorometer (Life Technologies Ltd, Paisley, UK) and Agarose gel electrophoresis. While RNA concentration and integrity were measured in a NanoDrop ND-1000 spectrophotometer and assessed through the Bioanalyzer 2010 instrument (Agilent Technologies, Palo Alto, CA, USA).

A total of 61 non-normalized libraries for RNA sequencing experiments were prepared by using SureSelect Strand Specific RNA-Seq Library Preparation kit (Agilent Technologies) and a single end sequencing (50SE) was carried out on an Illumina HiSeq2500 (Illumina Inc., San Diego, CA, USA). Raw Illumina sequencing data are deposited on SRA database (GenBank) under accession numbers SRP137798. All Illumina reads were analyzed with FastaQC software in order to assess sequence quality.

Array Comparative Genomic Hybridization

In total, the DNA obtained from 50 cDLBCL specimens paired with normal counterpart were analyzed using a 180,000-feature SurePrint G3 Canine CGH Microarray (4x180K, Agilent Technologies), as previously described [2]. Raw and normalized fluorescence data of all microarray experiments have been deposited in the GEO database (www.ncbi.nlm.nih.gov/geo/) under accession number GSE113258.

Methyl-CpG-binding (MBD) sequencing

Both for cDLBCLs and controls, methylated DNA was enriched by the MethylMiner Methylated DNA Enrichment Kit (Life Technologies) according to manufacturer's instructions. Briefly, 2 µg of genomic DNA was sonicated, using Covaris S2 (Covaris, MA, USA), to obtain fragments ranging from 200 to 600 bp in size and captured by MBD proteins. The methylated fraction of genomic DNA (100 ng) thus obtained was then employed to construct barcoded DNA libraries by using the TruSeq Nano DNA LT Library Prep Kit (Illumina Inc.) and sequenced with HiSeq2500 instrument (Illumina Inc.) following a 50 SE approach. Raw Illumina sequencing data are deposited on SRA database (GenBank) under accession numbers SRP137788.

Immunohistochemical score

For PD-L1 and CTLA-4, immunohistochemical scoring was recorded as the percentage of positive tumor cells over total tumor cells in the denominator (TPS), as reported by Roach et al. [3]. PD-L1 expression was only considered when positive on the membrane of neoplastic lymphocytes. PD-L1

surface membrane expression detected on macrophages and small lymphocytes infiltrating the tumor was not considered. For PD-1 and CD5, tumor infiltrating lymphocytes positive labeled were counted using Image Pro-Plus software after low-magnification scansion of 10 representative fields at magnification x400. The result was expressed as the average of positive cells/x400. For statistical analysis a 50% cut-off TPS for PD-L1 and CTLA-4 immunohistochemical results was used. While for PD-1 and CD5, DLBCLs were classified as having either less than or more than 30 positive tumor infiltrating lymphocytes/x400 field.

Data Mining

RNA-Seq raw reads from library sequencing were mapped to the CanFam3.1 genome assembly (Broad Institute, Cambridge, MA; released Sep. 2011; downloaded from the Ensemble Genome Browser site) using the software tool STAR [4]. Next, we obtained counts of aligned reads per gene using htseq-count from the HTSeq software package [5] in single-stranded mode, with canine gene annotations from Ensembl Release 87. Only reads that were uniquely aligned were retained. Differential expression analysis was performed using EdgeR. Deregulated expression of genes was considered as significant when $p<0.05$ (FDR corrected) was observed. To find sources of similarity in the dataset consisting of all 61 samples and the expression values of expression-filtered genes, multidimensional scaling (MDS) was applied. In the analysis, hierarchical clustering was used [6]. The stability of the identified clusters was assessed using consensus clustering [7]. To identify functional categories of differentially expressed genes, Gene Set Enrichment Analysis (GSEA) [8] was performed using the Java GSEA implementation. MBD-seq sequence reads were aligned to the CanFam3.1 genome (Ensembl Release 87) using Bowtie2 [9]. Quality and validity check of the mapped methylation-CpG binding reads was performed and high quality sequence data (MPS≥10) were analyzed using the MEDIPS software package to estimate methylation levels [10]. We calculated the short read coverage (extend value=300) at genome-wide 100-bp bins. Differential methylation analysis was carried out in 300 bp windows excluding regions with no read coverage. Genomic regions with at least one consecutive window that were statistically significantly differentially methylated ($p\leq0.001$) between compared samples were considered to be differentially methylated regions (DMRs). DMRs were annotated to the canine genome with respect to gene features using HOMER annotatePeaks script. If a peak had two or more annotations, a priority was assigned based on the order from left to right.

Copy number variations (CNVs) data were analyzed as previously described [2]. The comparison of transcriptomes with CNVs was done using a modified GEDI algorithm as previously described by Lenz et al. [11]. Deletions in Chr 26 and Chr 17, detected in 41 and 40 dogs out of 50 dogs, respectively, and concurrent in 33 animals, encompassed the IGLλ and IGLK genes. Deletions in Chr 8, seen in 35 dogs, encompassed the *IGHV* gene. Since these three recurrent aberrations likely reflected the normal immunoglobulin genes rearrangement they were discarded for further analyses. The impact of deletions, gains and amplifications of the selected genes on their own expression level was evaluated by comparing the average gene expression levels of deleted, duplicated and normal samples using Student's t-test. To assess the correlation between RNA-Seq and MBD-seq, the correlation coefficient r was calculated and normalized to stabilize variance by applying Fisher's Z-transformation [12].

Overall survival (OS) was defined as the time from diagnosis to death. Event-free survival (EFS) was defined as the time from starting therapy to the date of any diagnosed relapse. Chi-square method was used for categorical variables and Student's T-test for continuous variables. Survival was estimated with the Kaplan-Meier method and compared by log-rank tests. P values less than 0.05 were considered statistically significant. Multivariate Cox regression analysis was used to assess the independent prognostic impact of different variables in terms of EFS and OS. The P values for multiple comparisons were adjusted using the Benjamini–Hochberg correction. Statistical analyses were carried out with R software v3.1.3.

Cell lines, small interfering RNAs and cell transfection

CLBL-1 cell line was kindly provided by Dr Barbara Rutgen (University of Wien). CLBL-1 was maintained in IMDM 10% FBS. Rational siRNA design was performed by Sfold, which consider

target accessibility and RNA duplex thermodynamics. The siRNAs were purchased from Ambion (Thermo Fisher Scientific) and sequences are shown in Table S8. Cells were electroporated with 200 pmol of each siRNAs using Nucleofector in SG solution and the protocol DS142 was chosen. Nucleofection efficiency was checked by FACS after 24h electroporation by fluorescent labelled control siRNA, BLOCK IT (200 pmol). Propidium iodide was used to check cell viability. RNA was extracted at 24h, 48h and 72h.

Reverse-Transcriptase Polymerase Chain Reaction (RT-PCR)

CLBL-1 total RNA was purified by phenol:chloroform extraction. RNA was also treated with DNase I (Qiagen) to remove genomic DNA. Quantitative RT-PCR (qRT-PCR) was performed using Qiagen One-Step RT-PCR kit (Qiagen) on ABI Step One Plus (Applied Biosystems) and primers for LIN28B and MYC indicated in *Online Supplementary Table S8*. qRT-PCR data were analyzed using $\Delta\Delta$Ct and normalized. The housekeeping CCZ1 was used as reference gene [13].

MTT proliferation assay

CLBL-1 was exposed to increasing doses of compounds as previously described [14]. Bimiralisib was kindly provided by Piqur Therapeutics (Basel, Switzerland), MZ1 was synthesized as previously described [15] and the other compounds were acquired from Selleck Chemicals (Houston, TX). Total RNA was extracted at different time points.

***In vivo* experiment**

Fifteen NOD-Scid (NOD.CB17-Prkdcscid/NCrHsd) mice were purchased from Harlan Laboratory (five-six weeks of age, approximately 20 g body weight). Mice maintenance and animal experiments were performed under institutional guidelines established for the Animal Facility of the Institute of Research in Biomedicine (Bellinzona, Switzerland) and with study protocols approved by the local Cantonal Veterinary Authority. Mice were subcutaneously engrafted with of the canine lymphoma cell line CLBL-1 (10 x10^6 cells in 0.1mL of PBS) and divided into three experimental groups. Starting with an average tumor volume of 40 mm3, mice underwent treatment with bimiralisib and with MZ1 while controls received vehicle only. Bimiralisib was prepared in 20% SBECD (sulfobutyl-ether-β-cyclodextrin, Captisol, Dexolve) in water and pH was adjusted to 3.1. Application volume was 10 mL/kg and mice received through oral gavage (p.o.) 100 mg/Kg of bimiralisib every day for one week. MZ1 was prepared in 25% HP-ß-CD [(2-Hydroxypropyl)-β-cyclodextrin; Sigma Aldrich, MO, USA] in water and pH was adjusted to 6.2. Application volume was 5 mL/kg and mice were injected intraperitoneally (i.p.) with 100 mg/Kg of MZ1 every day for one week. Tumor size was measured as previously described [16].

Immunohistochemistry

Paraffin blocks obtained by formalin fixed tumor samples were cut into 5 µm sections on superfrost slides. Briefly, slides were placed in 70°C paraffin oven for 1 hour before deparaffinized in xylene and then rehydrated in 100%, 90%, 70% alcohol, successively. Antigen was retrieved by citric acid buffer (pH 6.0) in the 95°C water bath for 20 minutes. Endogenous peroxidase was inactivated by incubation in 3% H2O2 for 15 minutes. Following a pre-incubation with 10% normal goat serum to block nonspecific sites for 30 minutes, the sections were incubated with primary antibodies at room temperature for 30 minutes (anti-bovine PD-L1 monoclonal antibody, 5A2-A1, was diluted with PBS at 1:100, goat polyclonal anti-PD1 antibody, ab36151, at 1:100, mouse monoclonal anti-CTLA-4, ANC152.2, at 1:100, and mouse monoclonal anti-CD5, YKIX322.3, at 1:50). After the sections were washed with PBS twice for 5 minutes, positive staining was visualized with 3-diaminobenzidine tetrahydrochloride (DAB) according to manufacturer's protocol.

ONLINE SUPPLEMENTARY REFERENCES

1. Marconato L, Frayssinet P, Rouquet N, et al. Randomized, placebo-controlled, double-blinded chemoimmunotherapy clinical trial in a pet dog model of diffuse large B-cell lymphoma. Clin Cancer Res. 2014;20(3):668-677.
2. Arico A, Ferraresso S, Bresolin S, et al. Array-based comparative genomic hybridization analysis reveals chromosomal copy number aberrations associated with clinical outcome in canine diffuse large B-cell lymphoma. PLoS One. 2014;9(11):e111817.

3. Roach C, Zhang N, Corigliano E, et al. Development of a Companion Diagnostic PD-L1 Immunohistochemistry Assay for Pembrolizumab Therapy in Non-Small-cell Lung Cancer. Appl Immunohistochem Mol Morphol. 2016;24(6):392-397.
4. Dobin A, Davis CA, Schlesinger F, et al. STAR: ultrafast universal RNA-seq aligner. Bioinformatics. 2013;29(1):15-21.
5. Anders S, Pyl PT, Huber W. HTSeq--a Python framework to work with high-throughput sequencing data. Bioinformatics. 2015;31(2):166-169.
6. Eisen MB, Spellman PT, Brown PO, Botstein D. Cluster analysis and display of genome-wide expression patterns. Proc Natl Acad Sci U S A. 1998;95(25):14863-14868.
7. Monti S, Savage KJ, Kutok JL, et al. Molecular profiling of diffuse large B-cell lymphoma identifies robust subtypes including one characterized by host inflammatory response. Blood. 2005;105(5):1851-1861.
8. Subramanian A, Tamayo P, Mootha VK, et al. Gene set enrichment analysis: a knowledge-based approach for interpreting genome-wide expression profiles. Proc Natl Acad Sci U S A. 2005;102(43):15545-15550.
9. Langmead B, Salzberg SL. Fast gapped-read alignment with Bowtie 2. Nat Methods. 2012;9(4):357-359.
10. Weber M, Davies JJ, Wittig D, et al. Chromosome-wide and promoter-specific analyses identify sites of differential DNA methylation in normal and transformed human cells. Nat Genet. 2005;37(8):853-862.
11. Lenz G, Wright GW, Emre NC, et al. Molecular subtypes of diffuse large B-cell lymphoma arise by distinct genetic pathways. Proc Natl Acad Sci U S A. 2008;105(36):13520-13525.
12. Woo HG, Choi JH, Yoon S, et al. Integrative analysis of genomic and epigenomic regulation of the transcriptome in liver cancer. Nat Commun. 2017;8(1):839.
13. Giantin M, Aresu L, Arico A, et al. Evaluation of tyrosine-kinase receptor c-KIT (c-KIT) mutations, mRNA and protein expression in canine leukemia: might c-KIT represent a therapeutic target? Vet Immunol Immunopathol. 2013;152(3-4):325-332.
14. Boi M, Gaudio E, Bonetti P, et al. The BET Bromodomain Inhibitor OTX015 Affects Pathogenetic Pathways in Preclinical B-cell Tumor Models and Synergizes with Targeted Drugs. Clin Cancer Res. 2015;21(7):1628-1638.
15. Zengerle M, Chan KH, Ciulli A. Selective Small Molecule Induced Degradation of the BET Bromodomain Protein BRD4. ACS Chem Biol. 2015;10(8):1770-1777.
16. Tarantelli C, Gaudio E, Arribas AJ, et al. PQR309 Is a Novel Dual PI3K/mTOR Inhibitor with Preclinical Antitumor Activity in Lymphomas as a Single Agent and in Combination Therapy. Clin Cancer Res. 2018;24(1):120-129.
17. Charoentong P, Finotello F, Angelova M, et al. Pan-cancer Immunogenomic Analyses Reveal Genotype-Immunophenotype Relationships and Predictors of Response to Checkpoint Blockade. Cell Rep. 2017;18(1):248-262.

SUPPLEMENTARY TABLES

Supplementary Table S1. Differential expression analysis between cDLBCLs and normal lymph nodes. Columns A-C: Dog gene IDs (Ensembl and Entrez) and gene symbols. Column D: Gene type. Columns E,F: corresponding human gene IDs and gene symbols. Column G: likelihood ratio (LR) statistics. Column H: average logCPM (count-per-million) across all samples. Column I: logFC (Fold-change) between cDLBCLs and normal lymph nodes. Columns J-K: nominal and BH-adjusted (FDR) p-value.

Supplementary Table S2. Differential expression analysis between CLBL-1 cell line and normal lymph nodes. Columns A-C: Dog gene IDs (Ensembl and Entrez) and gene symbols. Column D: Gene type. Columns E,F: corresponding human gene IDs and gene symbols. Column G: likelihood ratio (LR) statistics. Column H: average logCPM (count-per-million) across all samples. Column I: logFC (Fold-change) between CLBL-1 and normal lymph nodes. Columns J-K: nominal and BH-adjusted (FDR) p-value.

Supplementary Table S3. Genes found differentially expressed in chromosomal regions with aberrations (Gains and Losses). Columns A-B: Dog gene IDs (Ensembl) and gene symbols. Column C: logFC (Fold-change) between cDLBCLs and normal lymph nodes. Columns D: BH-adjusted (FDR) p-value. Column E: Gene type.

Supplementary Table S4. Regions found differentially methylated between cDLBCLs and normal B-cells. Table S5 contains four worksheets organized as follow: **S2.1** Genomic regions significantly hypomethylated in cDLBCL compared to normal lymph nodes; **S2.2** Gene Set Enrichment Analysis (GSEA) of hypomethylated genes; **S2.3** Genomic regions significantly hypermethylated in cDLBCL compared to normal lymph nodes; **S2.4** GSEA of hypermethylated genes.

Supplementary Table S5. Differential expression analysis between cDLBCL1 and cDLBCL2. Columns A-C: Dog gene IDs (Ensembl and Entrez) and gene symbols. Column D: Gene type. Columns E,F: corresponding human gene IDs and gene symbols. Column G: likelihood ratio (LR) statistics. Column H: average logCPM (count-per-million) across all samples. Column I: logFC (Fold-change) between cDLBCLs and normal lymph nodes. Columns J-K: nominal and BH-adjusted (FDR) p-value.

Supplementary Table S6. Univariate and multivariate Cox regression analysis of overall survival for PD-L1 and PD-1 immunohistochemistry.

	Univariate Analysis			Multivariate Analysis		
	HR	**95% CI**	**P value**	**HR**	**95% CI**	**P value**
PD-L1 negative	0.446	0.234-0.765	0.006	0.505	0.274-0.956	0.036
PD-L1 positive	1					
PD-1 negative	0.551	0.351-1.155	0.024	0.945	0.301-1.452	0.041
PD-1 positive	1					
Age (<10 years)	0.765	0.541-1.575	0.397			
Age (>10 years)	1					
Stage (1-4)	1.542	0.884-3.553	0.145			
Stage (5)	1					
Substage a	1.753	1.054-2.563	0.021	2.405	1.309-4.794	0.011
Substage b	1					
Bone Marrow Infiltration neg	1.899	1.452-2.463	0.014	2.422	1.804-2.941	0.021
Bone Marrow Infiltration pos	1					

Supplementary Table S7 Sequences of siRNAs targeting LIN28B and primer sequences for LIN28B and MYC gene expression analysis by qRT-PCR.

siRNA sequences

siRNA	SENSE STRAND	ANTISENSE STRAND
LIN28Bex3	GGAUUCAUCUCCAUGAUAATT	UUAUCAUGGAGAUGAAUCCTT
LIN28B ex4	UGAAUCAAUACGGGUAACUTT	AGUUACCCGUAUUGAUUCATT

LIN28B and MYC primer sequences

PRIMER	FORWARD	REVERSE
LIN28B	CCTTGGATATTCCAGTCGATGT	TGGTTCTCCTTCTTTTAGGCTTCTA
MYC	TCCTCGGACTCTCTGCTCTC	TCAATTTCTTCTTCGTCCTCTTG

SUPPLEMENTARY FIGURES

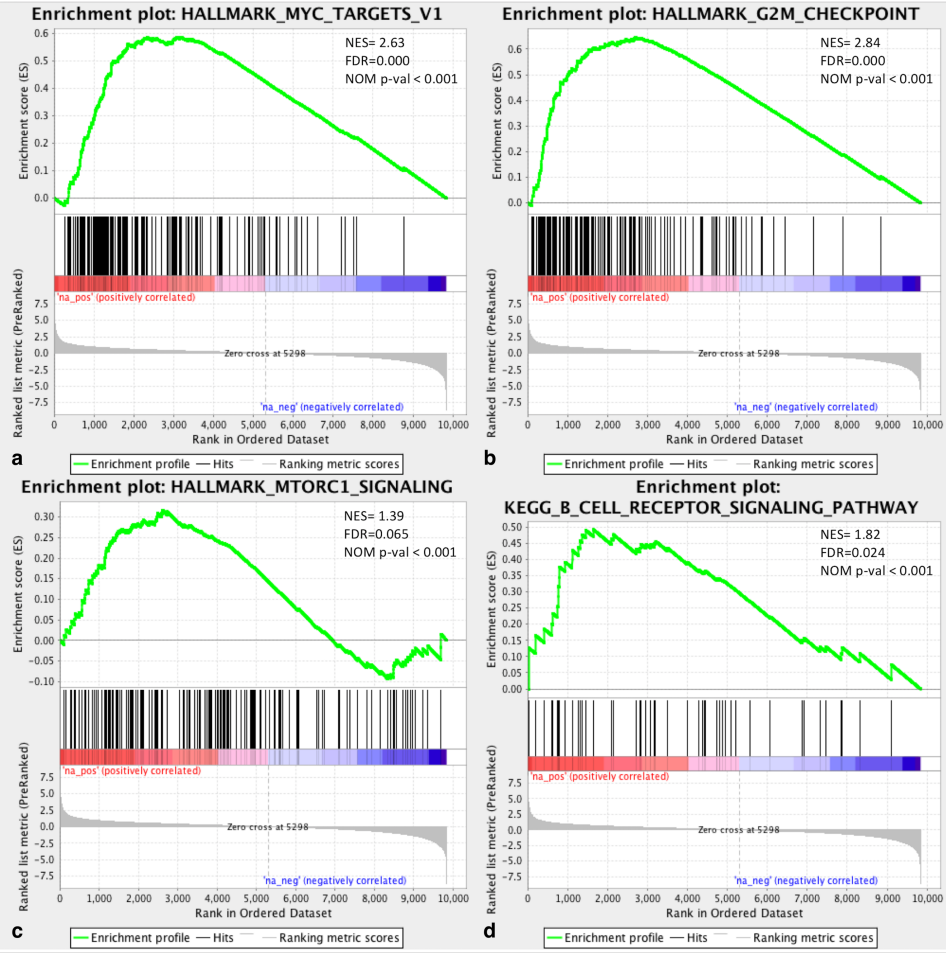

Supplementary Figure S1. GSEA plots for gene-expression signatures obtained in canine DLBCL compared to normal B-cells. Enrichment plots of MYC-targets **(a)**, G2M checkpoint **(b)**, MTORC1 signaling **(c)** and BCR signaling pathway **(d)**. Top, upregulated genes; bottom, downregulated genes. Green line, enrichment score; bars in the middle portion of the plots show where the members of the gene set appear in the ranked list of genes; Positive or negative ranking metric indicates, respectively, correlation or inverse correlation with the profile; NES, normalized enrichment score.

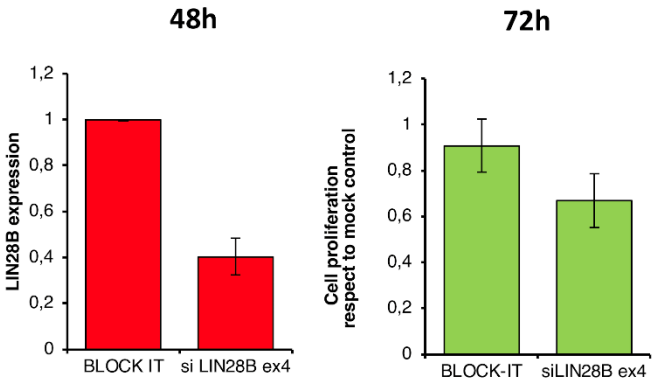

Supplementary Figure S2. LIN28B mRNA expression after 48h from transfection with LIN28B ex4 siRNA (*si LIN28B ex4*) compared to control (*BLOCK-IT*) (left panel). Cell viability after 72h from nucleofection with LIN28B ex4 siRNA (*si LIN28B ex4*) compared to control (*BLOCK-IT*) measured by MTT assay (right panel). Results are expressed as average of three independent experiments.

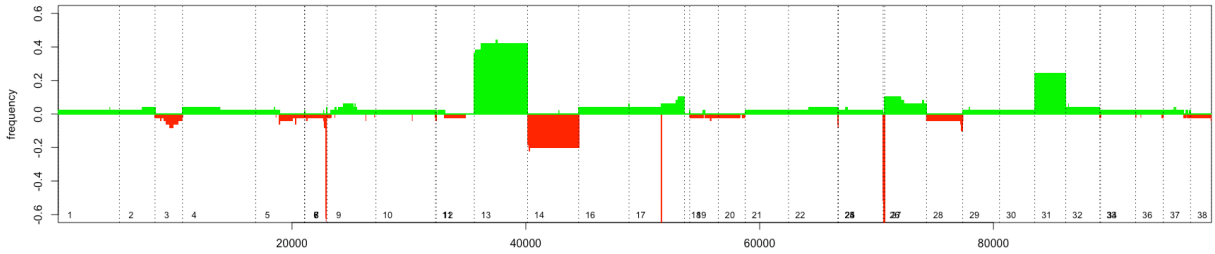

Supplementary Figure S3. **Frequency plots of DNA gains (green) and losses (red) observed in 50 canine DLBCLs.** X axis: chromosome localization and physical mapping. Y axis: percentage of cases bearing the aberration.

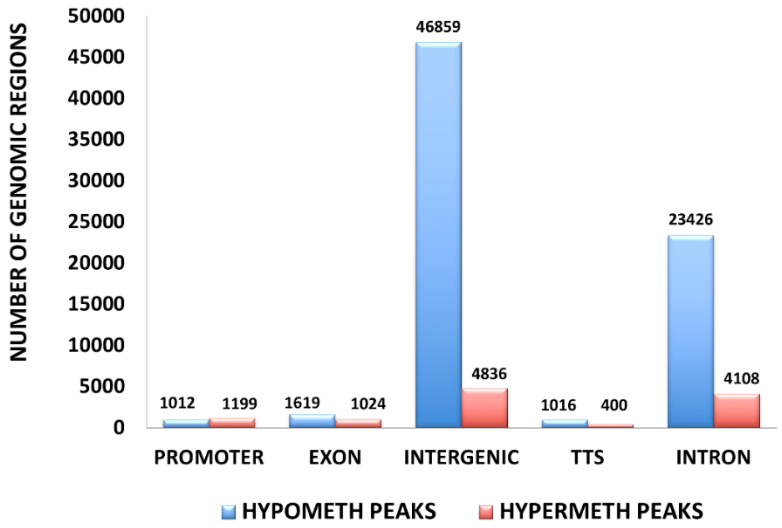

Supplementary Figure S4. Bar plots showing the number of differentially methylated peaks in canine DLBCL compared with normal B-cells. Results are reported separating peaks according to genomic locations.

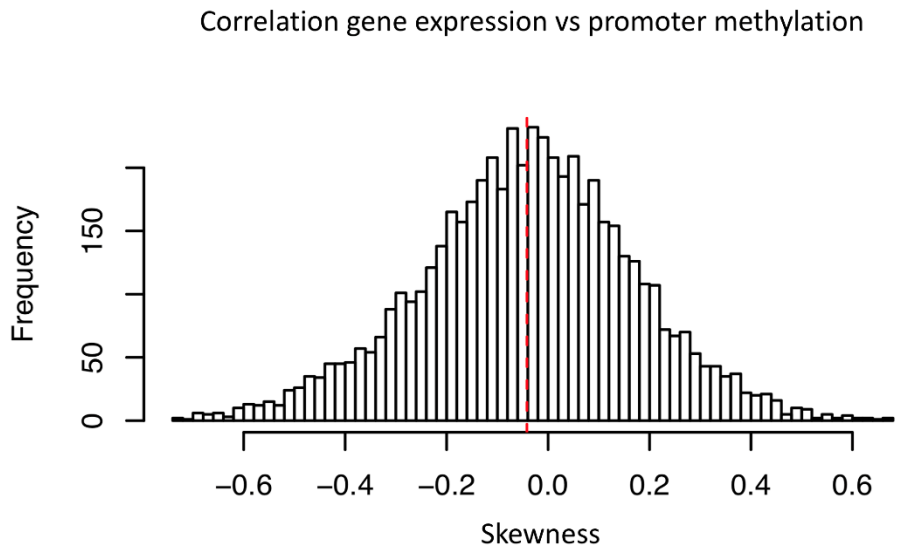

Supplementary Figure S5. Histogram and skewed distribution showing a negative correlation between the differences in mRNA expression and promoter methylation (skewness= -0.06, *P* <0.01). The red line represents a linear regression.

A

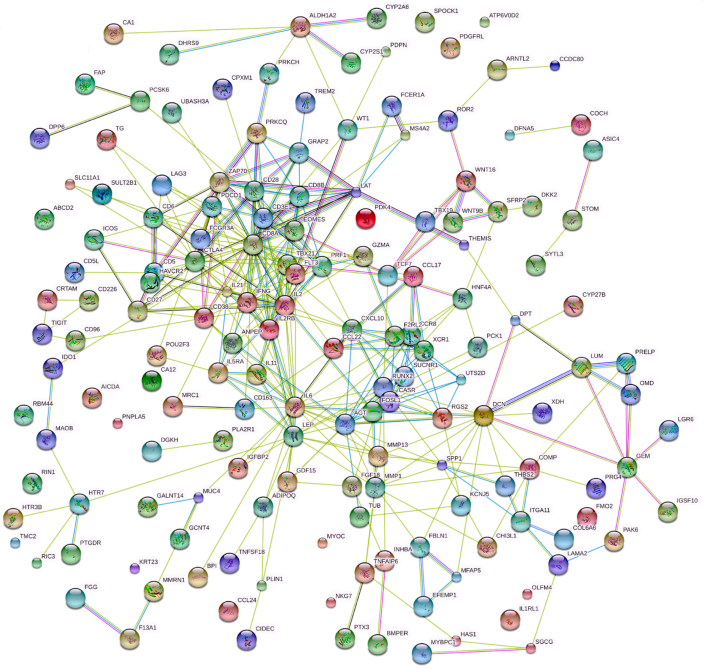

B

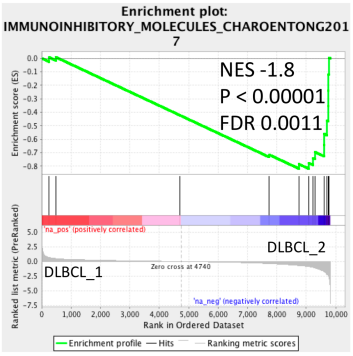

Supplementary Figure S6. Functional analysis of genes significantly up-regulated in DLBCL_2 compared to DLBCL_1. A. Representative protein-protein interaction network of genes generated from STRING database. The connecting lines indicate functional relationships and direct protein-protein interactions. B. GSEA plot for gene-expression signatures obtained in DLBCL_1 compared to DLBCL_2 and then analyzed for their enrichment in immunoinhibitory molecules as reported by Charoentong et al. [17]. Green line, enrichment score; bars in the middle portion of the plots show where the members of the gene set appear in the ranked list of genes; Positive or negative ranking metric indicates, respectively, correlation or inverse correlation with the profile; NES, normalized enrichment score.

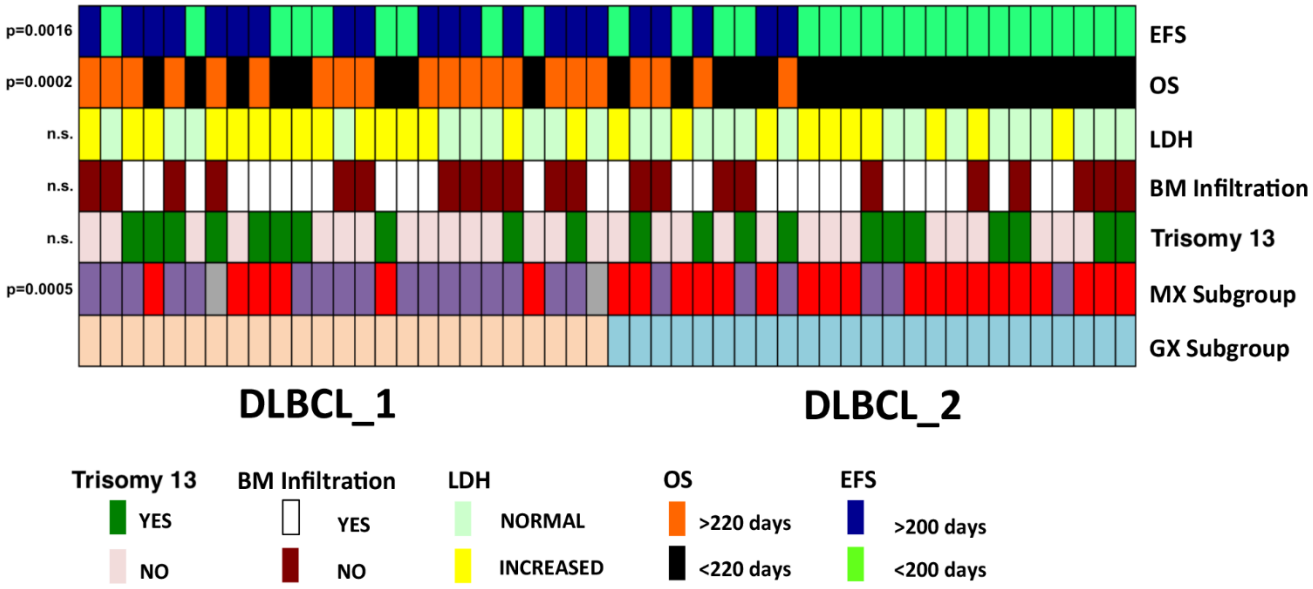

Supplementary Figure S7. Clinical, molecular and genotypic features of cDLBCLs. Tumor subgroups identified by RNA-seq (GX Subgroup) are indicated in salmon (DLBCL_1) and light blue (DLBCL_2) bars; methylation subgroups (MX Subgroup) obtained by unsupervised clustering are indicated in violet (group 1), red (group 2) and grey (group 3). Trisomy of chromosome 13, bone marrow (BM) infiltration, LDH, Overall Survival (OS) and Event Free Survival (EFS) in individual tumors are indicated. Significant correlation between clinical/molecular features and GX subgroups are reported on the left.

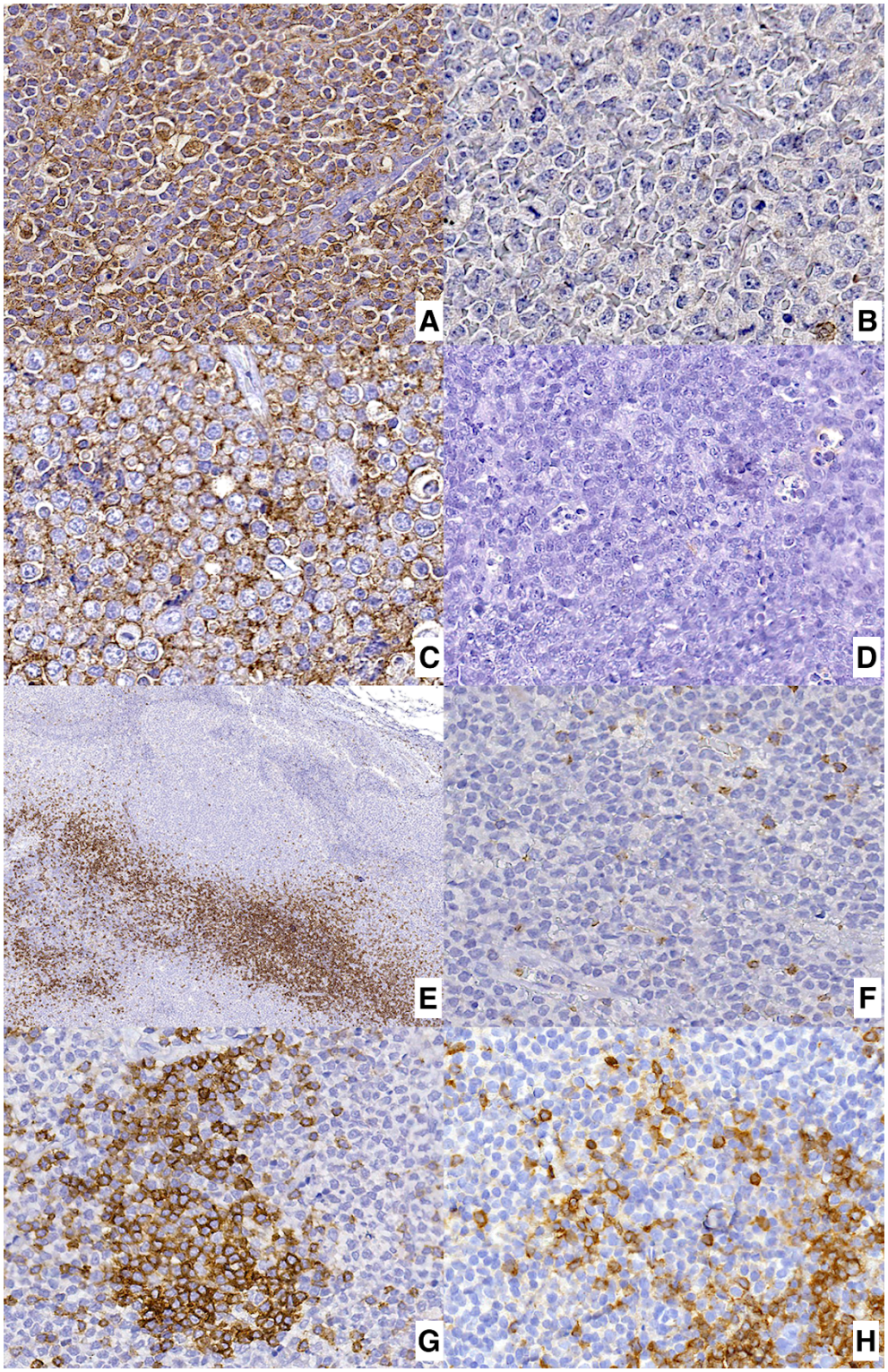

Supplementary Figure S8. Representative immunohistochemical analysis of PD-L1, CTLA-4, PD-1 and CD5 expression in cDLBCL. (A) PD-L1 positive tumor cells in cDLBCL. (B) PD-L1 negative tumor cells in cDLBCL. (C) CTLA-4 positive tumor cells in cDLBCL. (D) CTLA-4 negative tumor cells in cDLBCL. (E) PD-1 lymphocytes in cDLBCL. (F) Small number of PD-1 lymphocytes in cDLBCL. (G) CD5 lymphocytes in cDLBCL. (H) Small number of CD5 lymphocytes in cDLBCL.

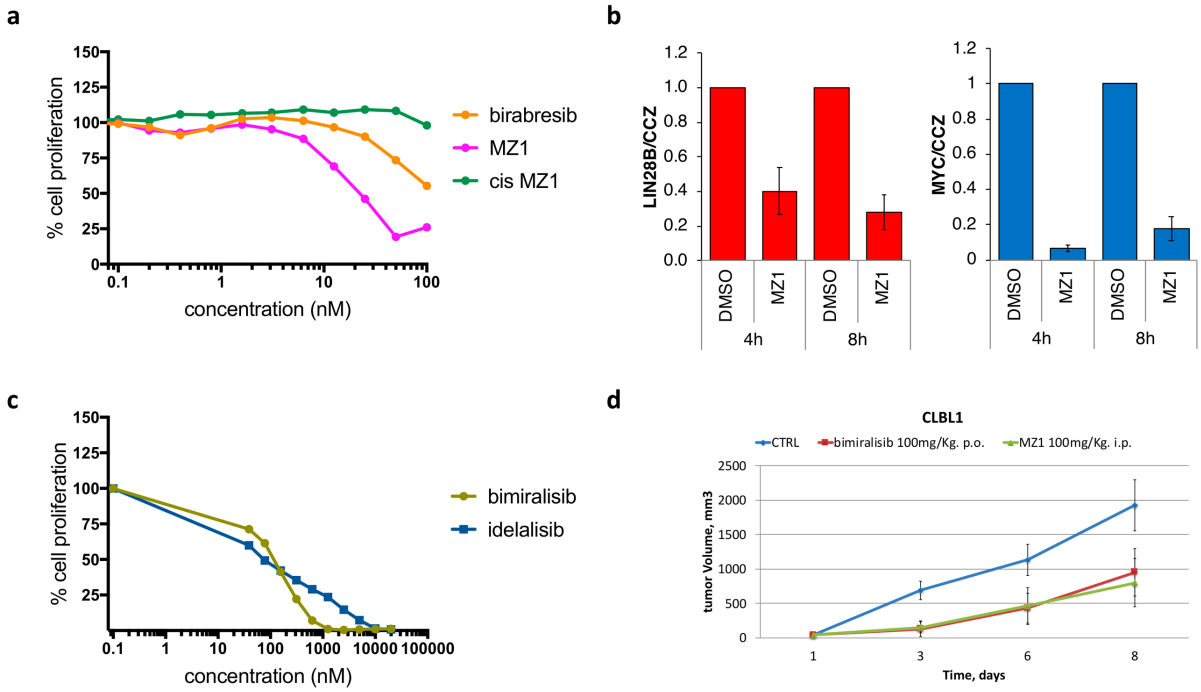

Supplementary Figure S9. Activity of targeted molecules on CLBL1 cell line. (a) CLBL1 cell line was exposed to increased doses of birabresib (OTX015/MK-8628), MZ1 or cis MZ1 for 72 hours. Anti-proliferative activity was evaluated by MTT assay. **(b)** CLBL1 cell line was treated with DMSO or MZ1 (500 nM) for 4 and 8 hours and expression of LIN28B (left) or MYC (right) was evaluated by Real Time-PCR. **(c)** CLBL1 cell line was exposed to increased doses of bimiralisib (PQR309) or idelalisib for 72 hours. Anti-proliferative activity was evaluated by MTT assay. Results are expressed as average of three independent experiments. **(d)** NOD-SCID mice subcutaneously inoculated with the CLBL-1 cell line and treated with bimiralisib (n = 5), with MZ1 (n = 5) or vehicle control (CTRL, n = 5). Y-axis: Tumor volumes in mm3. X-axis, days post first treatment (Day 1).

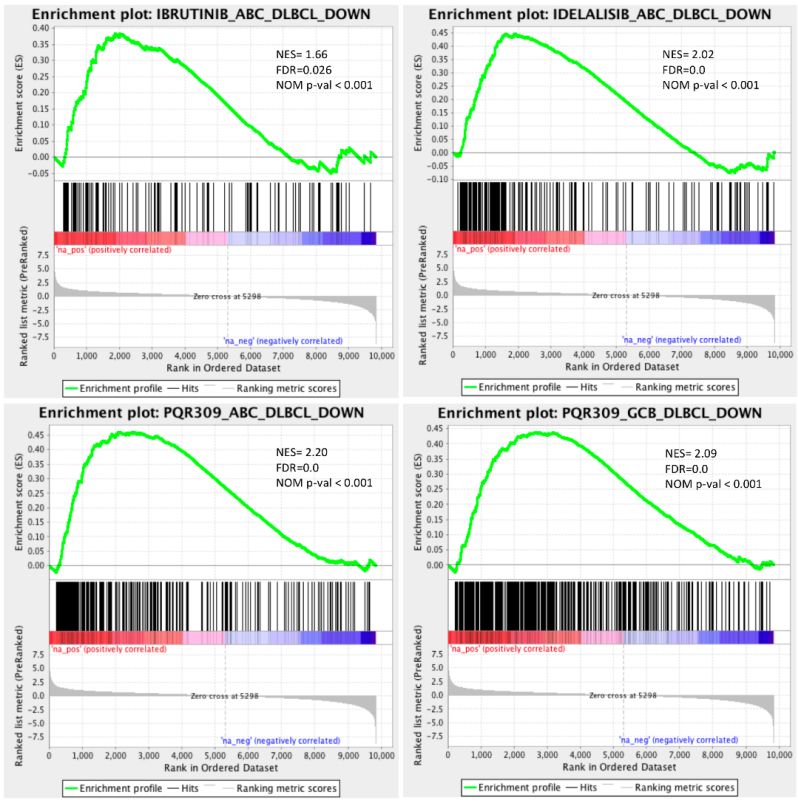

Supplementary Figure S10. GSEA plots for gene-expression signatures obtained in cDLBCL compared to controls and then analyzed for their enrichment in ibrutinib target genes (top left), idelalisib target genes (top right), and bimiralisib (PQR309) target genes in ABC-DLBCL (bottom left) as well as bimiralisib target genes in GC-DLBCL (bottom right), as defined by Tarantelli et al. [16]. Top, upregulated genes; bottom, downregulated genes. Green line, enrichment score; bars in the middle portion of the plots show where the members of the gene set appear in the ranked list of genes; Positive or negative ranking metric indicates, respectively, correlation or inverse correlation with the profile; NES, normalized enrichment score.